Ab initio study of permanent electric dipole moment and radiative lifetimes of alkaline-earth-metal–Li molecules

Geetha Gopakumar,[1] Minori Abe,[1] Masatoshi Kajita,[2] and Masahiko Hada[1]
[1]*Department of Chemistry, Tokyo Metropolitan University, 1-1 Minami-Osawa, Hachioji, Tokyo 192-0397, Japan*
[2]*National Institute of Information and Communication Technology, Nukui-Kitamachi, Koganei, Tokyo 184-795, Japan*
(Received 14 October 2011; published 28 December 2011)

We calculate permanent electric dipole moments (PDMs), as well as spontaneous and black body lifetimes, of alkaline-earth-metal–Li (AEM-Li) ultracold polar molecules to study anisotropic long-range dipole-dipole interactions in a single quantum state. We obtain potential energy curves for the $^2\Sigma$ ground state of MgLi, CaLi, SrLi, and BaLi molecules at the coupled cluster singles and doubles with partial triples [CCSD(T)] level of electron correlation. Calculated spectroscopic constants for the isotopes: $^{24}Mg^7Li$, $^{40}Ca^7Li$, $^{88}Sr^7Li$, and $^{138}Ba^7Li$, show good agreement with available theoretical and experimental results. We obtain PDM curves using finite field perturbation theory at the CCSD(T) level. We find that AEM-Li molecules have moderate values of PDM at the equilibrium bond distance (MgLi: 0.90 D, CaLi: 1.15 D, SrLi: 0.33 D, and BaLi: –0.42 D) and hence might be suitable candidates for the proposed study in a single quantum state. Radiative lifetime calculations of the $v = 0$ state ($^{24}Mg^6Li$: 22 s, $^{40}Ca^6Li$: 39 s, $^{88}Sr^6Li$: 380 s, and $^{138}Ba^6Li$: 988 s) are found to be longer than the typical time scale associated with ultracold experiments with these molecules. The uncertainty in the lifetime calculations are estimated to be less than 10%.

DOI: 10.1103/PhysRevA.84.062514 PACS number(s): 31.15.A−, 31.15.bw, 31.15.vn, 31.50.Bc

I. INTRODUCTION

Ultracold atoms have opened new fields of experimental quantum physics, such as Bose-Einstein condensation [1] and atom optics [2]. Using polar molecules, similar research offers exciting prospects for producing new types of quantum gases. Polar molecules interact with each other via highly anisotropic long-range electric-dipole-dipole forces [3,4]. They pave the way for new techniques in high-precision spectroscopic and scattering experiments, which in turn shed light on fundamental physical problems such as measurement of the electric dipole moment of an electron [5] and time variance of the proton–to-electron mass ratio [6,7].

Estimation of the permanent dipole moment (PDM) and the black body radiative lifetime are important factors in the study of interactions between ultracold molecules. This information leads to valuable insights into the stability of a Bose-Einstein condensate and the Fermi degeneracy in a single quantum state. Due to the large PDM of bi-alkali-metal polar molecules (KRb [8,9], NaLi [10], NaCs [11], RbLi [12], RbCs [13,14], CsLi [15,16]), previous studies on dipole-dipole interactions and electric-field control in the ultracold regime were primarily centered around bi-alkali-metal polar molecules. Alkali-metal–Li molecules, such as NaLi [10], RbLi [12], and CsLi [15,16], have already been cooled to temperatures in the ultracold regime and have been produced in their electronic ground states through photoassociation [17] and Feshbach resonance [18] techniques. However, in order to manipulate molecules to achieve quantum degeneracy in the absolute ground state, molecules should be localized in a single quantum state, defined by their vibrational, rotational, and hyperfine structure. The lifetime in this localized state must be sufficiently long. Alkali-metal–Li molecules are not advantageous to localize in a single quantum state because their hyperfine structure is complicated due to the nonzero nuclear spins of both alkali-metal and Li atoms. In addition, it is difficult to split the hyperfine substates in the presence of magnetic field due to the small Zeeman effect in their $^1\Sigma$ states. Lastly, alkali-metal–Li molecules are not advantageous systems in which to achieve long lifetimes of a single quantum state because the perturbation induced by black body radiation is significant due to the large values of PDM, as in the case of more than three debye.

Apart from bi-alkali-metal polar molecules, studies on other possible species, such as alkali-metal–lanthanide (RbYb [19], LiYb [20–22], SrYb [23]) and lanthanide dimers (Sr_2 [24],Yb_2 [25]), have been reported. A recent proposal for the precise measurement of vibrational transition frequencies of alkaline-earth-metal–H ionic polar molecules [26,27] reiterates the importance of investigations regarding ultracold polar molecules. Furthermore, theoretical investigations of the structure of polar alkali-metal–Sr (LiSr, NaSr, KSr, RbSr, and CsSr) diatomic molecules [28] have been made, resulting in the realization of samples of new species in the ultracold regime.

AEM-Li molecules are attractive systems to study in the ultracold regime, because Li is the lightest atom that can be cooled in the ground state and therefore their vibrational and rotational transition frequencies are largest among the ultracold molecules. Additionally, there are four other important advantages in considering the following species: (i) The PDMs of AEM-Li molecules are small and hence are experimentally advantageous, since it is possible to keep the molecules in the single quantum state for a long period. (ii) The nuclear spin of even isotopes of alkaline-earth-metal atoms is zero and the hyperfine energy structure of AEM-Li molecules is much simpler than for bi-alkali-metal molecules. (iii) It is much easier to split the hyperfine sublevels in the presence of a magnetic field than it is for alkali-alkali molecules in the $^1\Sigma$ state. (iv) By choosing ^{6}Li (fermion) or ^{7}Li (boson), AEM-^{6}Li (fermionic) and AEM-^{7}Li (bosonic) molecules can be selectively produced.

In this paper we present ground-state potential energy curves and PDMs of AEM-Li molecules using coupled cluster singles and doubles with partial triples [CCSD(T)] with relativistic correlation-consistent atomic natural orbital (ANO-RCC) [29] basis sets. CCSD(T) is the best method for the AEM-Li type of molecules because the ground states can be written with a single configuration over the entire potential curve. To check the accuracy of our computed potential energy curves, we have compared the ground-state spectroscopic constants with available theoretical and experimental values. Electronic PDM functions and parallel dipole polarizabilities are obtained using the finite field perturbation theory (FFPT) with CCSD(T) energy calculations. Last but not least, we calculate the vibrational levels of the ground electronic states. Using the PDM functions, we compute the spontaneous and black body radiative lifetimes for each of these levels in the presence of thermal black body radiation.

II. CALCULATION DETAILS

Throughout this study we employed the MOLCAS version 7.2 program packages to execute all of the calculations [30]. We assumed C_{2v} point-group symmetry. We took into account scalar relativistic effects through the third-order Douglas-Kroll-Hess (DKH) [31,32] transformation of the relativistic Hamiltonian. We have obtained potential energy curves and the corresponding spectroscopic constants at spin-free level, considering the fact that the ground-state spin-orbit effects are negligible for AEM-Li systems, as demonstrated with the YbLi molecule [20].

The electronic ground states of AEM-Li molecules and their corresponding equilibrium bond distances (R_e), dissociation energies (D_e), harmonic frequencies (ω_e), anharmonic constants ($\omega_e x_e$), and rotational constants (B_e) were obtained using the CCSD(T) method. In CCSD(T) calculations, all the core electrons below Mg($2s$), Ca($3s$), Sr($4s$), and Ba($4d$) are frozen and hence the excitations are taken to be from Li $1s, 2s$; Mg $2p, 3s$; Ca $3p, 4s$; Sr $4p, 5s$; and Ba $5s, 5p, 6s$ orbitals. We obtained electronic PDM functions and dipole polarizabilities by FFPT, taking dipole field strengths to be in the range $\pm 10^{-4}$ a.u. to $\pm 10^{-5}$ a.u., followed by numerical derivative analysis. In order to investigate the stability of ultracold molecules in the presence of a black body radiation field ($T = 300$ K), we obtained an estimation the black body radiation lifetimes of vibrational levels of the electronic $^2\Sigma$ ground state.

The ANO-RCC basis set types, along with the corresponding contraction styles, are tabulated in Table I. Basis set superposition error (BSSE) can be considered negligible, as demonstrated in our earlier paper [20] on LiYb systems using the largest ANO-RCC basis set. To obtain spectroscopic constants, we used the VIBROT package in MOLCAS with a wide range, between $R = 4.0$ and 50.0 a.u.,(1 a.u. = 0.529 Å), taking 500 grid points. For calculations of the vibrational PDM of the absolute ground state, a smaller range ($R = 4.0$–30.0 a.u.) with a dense grid (1000 points) was used. In both cases we used the maximum vibrational states associated with the $J = 0$ rotational state in order to fit the curve. To check the accuracy of the dipole polarizability calculations, we obtained supermolecular limit calculations at 100.0 a.u. and compared them with the respective atomic limits. We obtained radiative rates

TABLE I. ANO-RCC basis set contraction style and corresponding correlated orbitals.

Elements	Contraction style	Correlated orbitals
Li	$(14s9p4d3f1g)/[8s7p4d2f1g]$	$1s$,$2s$
Mg	$(17s12p6d2f)/[9s8p6d2f]$	$2p$,$3s$
Ca	$(20s16p6d4f)/[10s9p6d4f]$	$3p$,$4s$
Sr	$(23s19p12d4f)/[11s10p7d4f]$	$4p$,$5s$
Ba	$(26s22p15d4f)/[12s10p8d4f]$	$5s$,$5p$,$6s$

in the presence of black body (BB) radiation ($T = 300$ K) by computing the emission and absorption contributions [13] as

$$\Gamma_{\nu}^{\mathrm{BB}} = \sum_{\nu'} \bar{n}(\omega_{\nu'})\Gamma^{\mathrm{emis}}(\nu \to \nu') + \sum_{\nu''} \bar{n}(\omega_{\nu''})\Gamma^{\mathrm{abs}}(\nu \to \nu''), \tag{1}$$

where the indices ν' and ν'' denote vibrational levels with an energy that is smaller or larger than that of ν, respectively. The factor $\bar{n}(\omega)$ corresponds to the average number of photons in an electromagnetic mode at frequency ω and is given by

$$\bar{n}(\omega) = \frac{1}{e^{-\hbar\omega/k_B T} - 1}, \tag{2}$$

where $\hbar$ and k_B are the Planck's and Boltzmann constants. The spontaneous emission rate is given by

$$\Gamma_{\nu}^{\mathrm{spont}} = \sum_{\nu'} \Gamma^{\mathrm{emis}}(\nu \to \nu'), \tag{3}$$

where the indices ν' denote vibrational levels with an energy that is smaller than that of ν' The emission and absorption rates in the black body and spontaneous rate equations are proportional to the cube of energy difference between the vibrational states and square of the transition dipole moments

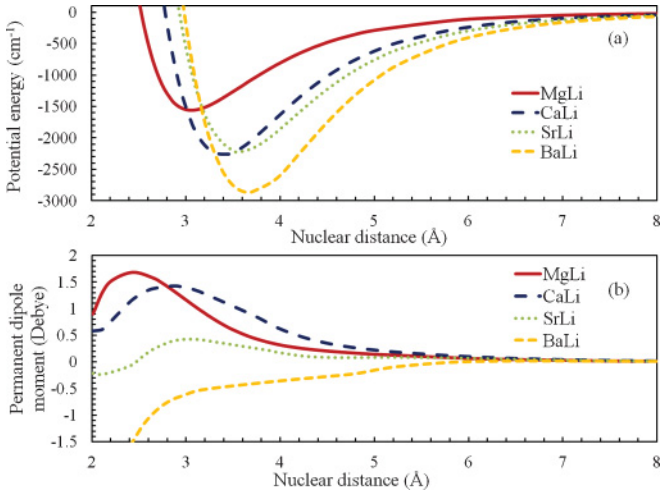

FIG. 1. (Color online) (a) Potential energy curves and (b) permanent dipole moments (PDM) of the ground $^2\Sigma$ state for AEM-Li molecules [AEM: Mg (thick red line), Ca (blue long dashed line), Sr (green dotted line), and Ba (orange short dashed line)] at CCSD(T) levels of correlation.

TABLE II. Spectroscopic constants for ground $^2\Sigma$ states of $^{24}Mg^7Li$, $^{40}Ca^7Li$, $^{88}Sr^7Li$, and $^{138}Ba^7Li$ at CCSD(T) level of correlation.

Molecule	Method	R_e (Å)	ω_e (cm^{-1})	$\omega_e x_e$ (cm^{-1})	B_e (cm^{-1})	α_e (cm^{-1})	D_e (eV)
MgLi	CCSD(T)	3.116	176.0	7.31	0.321	0.0123	0.165
	CASSCF-MRCI[a]	3.110	183	–	–	–	0.20
	CCSD(T)	3.395	196.7	4.85	0.246	0.005	0.280
	QCISD(T)[b]	3.410	194	–	–	–	0.27
CaLi	CASSCF-MRCISD[b]	3.400	204	–	–	–	0.27
	Experiment[b]	3.379	195.2	–	–	–	0.24
	CIPSI[c]	3.296	196.13	–	–	–	0.292
SrLi	CCSD(T)	3.531	182.1	4.29	0.203	0.004	0.276
	CIPSI[d]	3.480	184.9	–	0.210	–	0.321
BaLi	CCSD(T)	3.668	190.9	3.19	0.187	0.0023	0.356
	CIPSI[e]	3.589	200.8	3.20	0.198	0.0037	0.390

[a]Reference [33].
[b]Reference [34].
[c]Reference [35].
[d]Reference [36].
[e]Reference [37].

(TDMs) between them. This is given by

$$\Gamma^{\text{emis or abs}}(v \to v') = \frac{8\pi}{3}\frac{1}{\hbar c^3}\omega^3 |\langle v|d|v'\rangle|^2, \qquad (4)$$

where $|\langle v|d|v'\rangle|$ denotes the TDMs between vibrational states.

III. RESULTS AND DISCUSSION

A. Potential energy curves and spectroscopic constants

Figure 1(a) shows the potential energy curves acquired at the CCSD(T) level of electron correlation. These curves are drawn relative to the dissociation limit [AEM($^1S_0$) + Li($^2S_{1/2}$)] of each AEM-Li species, which has been computed at the bond distance of 100.0 a.u. In Table II we report the ground-state spectroscopic constants of AEM-^{7}Li (bosonic) molecules using the ANO-RCC basis sets at the CCSD(T) level. Previous theoretical and experimental data of the abundant bosonic (AEM-^{7}Li) species are listed together. For MgLi, the spectroscopic constant calculations at the CCSD(T) level compares very well with the available CASSCF-MRCI [33] calculations ($R_e \sim 0.01$ Å, $\omega_e \sim 7$ cm^{-1}, $D_e \sim 0.03$ eV). Experimental spectroscopic constants for MgLi are not available to our knowledge, whereas for CaLi, comparison between our calculations and experimental values by Russon *et al.* [34] shows R_e and ω_e to be accurate to 1%. At the same time, *ab initio* configuration interaction by perturbation selected iteration (CIPSI) calculations by Allouche and Aubert-Frecon [35] yield a shorter bond length (∼0.1 Å) in comparison with our CCSD(T) calculations and those obtained by experiment [35]. Calculations for dissociation energy by different correlation methods, including our CCSD(T) results, are found to be overestimated (∼0.04 eV) with respect to experiment. The theoretical calculation employing the CIPSI method is likewise reported for SrLi [36] and BaLi [37] molecules. This method reveals a similar trend (short bond length and large dissociation energy) as in the case of CaLi. Hence we can expect the error of present calculations on SrLi and BaLi molecules to be around 1%, as in the case of the CaLi molecule. Our spectroscopic data is a good theoretical reference, especially for the heavy molecules, because few reports exist at this point in time. In Fig. 1(a) we found a rough tendency for the binding energy to become larger and the bond length to become longer as the AEM atom becomes heavier.

Table III lists the calculated spectroscopic data for AEM-^{6}Li molecules at the CCSD(T) level. AEM-^{6}Li molecules are experimentally advantageous for the study of dipole-dipole interactions because the higher-order intermolecular interactions are suppressed for fermionic systems at ultralow temperatures. Note also that AEM-^{6}Li molecules are more advantageous than AEM-^{7}Li molecules for precision measurements of the vibrational transition frequency [38] because the g factor of ^{6}Li nuclear spin is smaller than that of ^{7}Li nuclear spin [39].

In Fig. 1(a), the dissociation energies of BaLi (2871 cm^{-1}), SrLi (2223 cm^{-1}), and CaLi (2260 cm^{-1}) are moderately large, providing molecular stability. To check whether these polar molecules are stable against collision in the ultracold environment, we have compared them with published theoretical

TABLE III. Spectroscopic constants for ground ($^2\Sigma$) states of $^{24}Mg^6Li$, $^{40}Ca^6Li$, $^{88}Sr^6Li$, and $^{138}Ba^6Li$ at CCSD(T) level of correlation.

Molecule	R_e (Å)	ω_e (cm^{-1})	$\omega_e x_e$ (cm^{-1})	B_e (cm^{-1})	α_e (cm^{-1})	D_e (cm^{-1})
MgLi	3.116	187.0	8.24	0.363	0.015	1332
CaLi	3.395	210.4	5.58	0.293	0.006	2260
SrLi	3.531	195.8	4.98	0.234	0.004	2223
BaLi	3.668	205.5	3.69	0.217	0.003	2871

and experimental dissociation energies of Ba_2 (1629 cm^{-1} [40]), Sr_2 (1061 cm^{-1} [41]), Ca_2 (1095 cm^{-1} [42]), and Li_2 (8517 cm^{-1} [43]) dimers. AEM-Li molecules would be stable provided that the stability condition $2D_e(\text{AEM} - \text{Li}) \gg D_e(\text{AEM}_2) + D_e(\text{Li}_2)$ is satisfied. Unfortunately, this condition is not well satisfied because of the large dissociation energy of the Li_2 molecule. One way to overcome this difficultly is to trap AEM-^{6}Li molecules in a single quantum state in a two-dimensional trap to suppress inelastic collisions. Using this method, Ospelkaus *et al.* [44] succeeded in suppressing the KRb + KRb dissociation to $K_2 + Rb_2$ reaction.

B. Permanent dipole moment, dipole polarizability, and radiative lifetimes

Figure 1(b) shows the PDMs as functions of internuclear distance R at the CCSD(T) level of correlation using the FFPT method. The dipole field strengths were chosen after a few tests were performed, taking care to reduce the discontinuities in the PDM functions (due to kinks in potential energy curves). The dipole field strength was finally chosen to be ± 0.00009 a.u. for all of the molecules. Also shown are the PDM graphs acquired at the Hartree-Fock (HF) level by the FFPT method and as expectation values in Figs. 2(a) and 2(b), respectively. These two figures are nearly identical, which implies that the FFPT calculations that rely on the chosen dipole field strength are appropriate and reliable.

For MgLi, CaLi, and SrLi, the PDM functions at the CCSD(T) level demonstrate similar behavior as a function of internuclear distance R, wherein the magnitude gradually increases as R decreases, reaches a maximum at $R < R_e$, and drops thereafter. The only available theoretical calculation for the PDM function by Guérout *et al.* [36] using the CIPSI algorithm for SrLi molecules also shows a similar trend as in our FFPT calculation. For BaLi, in contrast, the PDM curve at the CCSD(T) level does not exhibit such a maximum point, remaining entirely negative. This tendency comes about from electron correlation effects as understood from the maxima in the PDM curve of BaLi molecules at the HF level in Fig. 2. Large differences between the HF and CCSD(T) levels of correlation also appear in the PDM curves of MgLi. It is rather surprising that the electron correlation effects are significant in the PDM functions of AEM-Li systems. Hence, for the AEM-Li systems, simple analysis using electron negativity [21] or ionization energy [8,13] may not work to explain the tendency of PDM signs and values among the different molecules. We have obtained the PDM values at the equilibrium internuclear distance to be 0.90 D for MgLi, 1.15 D for CaLi, 0.33 D for SrLi, and –0.42 D for BaLi. These values, particularly for MgLi and CaLi, are reasonably large, making them good candidates for the study of long-range interactions Comparison of SrLi theoretical calculations by Guérout *et al.* [36] shows the PDM value at equilibrium internuclear distance to be 0.34 D at $R_e = 3.48$ Å as compared to 0.33 D at $R_e = 3.53$ Å using our FFPT calculation. Examining the accuracies of spectroscopic constants and PDM values at equilibrium internuclear distance, we infer that the potential energy curves and the subsequent PDM curves by FFPT are fairly accurate (∼3%).

In Table IV we show the parallel component of the static electric dipole polarizability at the equilibrium distance R_e,

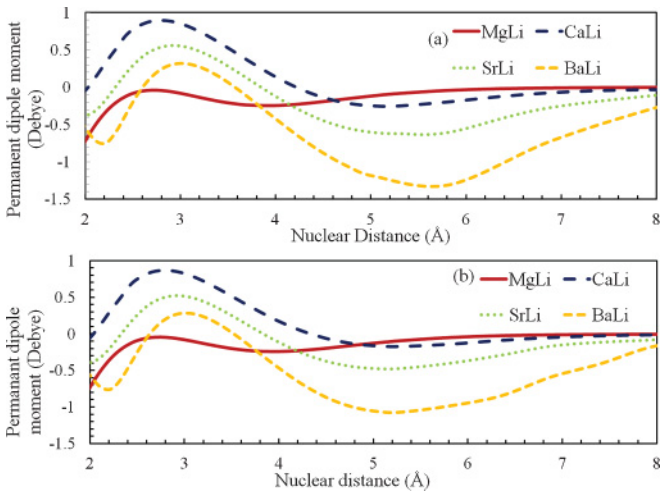

FIG. 2. (Color online) Permanent dipole moments (PDMs) of ground $^2\Sigma$ state at the Hartree-Fock level for AEM-Li molecules [AEM: Mg (thick red line), Ca (blue long dashed line), Sr (green dotted line), and Ba (orange short dashed line)] by (a) FFPT and (b) as an expectation value.

denoted α_{zz}. Moreover, we illustrate the supermolecular limits at the bond length of 100.0 a.u., denoted α_{100}. We calculated the values of α_A as $\alpha_{Li} + \alpha_{AEM}$, shown in Table IV, from the experimental dipole polarizabilities of atoms [45]. Our supermolecular data (α_{100}) is significantly close to the experimental values (α_A) for all the molecules (less than 1% error). Hence we infer the accuracy of the electric dipole polarizability calculations in the equilibrium internuclear region to be of similar order. The parallel electric dipole polarizability over the complete internuclear distance is given in Fig. 3. For all AEM-Li molecules, we find a gradual increase in dipole polarizability with respect to internuclear distance, reaching a maximum value at $R > R_e$, and then dropping to atomic dipole polarizability limits at large R values. The magnitude of the dipole polarizability increases gradually as we move from the MgLi to the BaLi molecule. These dipole polarizabilities are important parameters by which to understand the possibility of manipulating the direction of the molecular axis in the presence of electric field.

TABLE IV. Ground-state parallel dipole polarizability (α_{zz}) at equilibrium internuclear distance and supermolecular limits (100.0 a.u.) for AEM-Li molecules at CCSD(T) level of theory. Experimental and theoretical molecular dipole polarizabilities obtained as the sum of the dipole polarizabilities of the constituent atoms are compared with the dipole polarizability (α_{100}) obtained at $R =$ 100.0 a.u. Atomic dipole polarizability (α_A) of constituent atoms are obtained from Ref. [45] as follows: Li: 164.0 a.u., Mg: 71.3(7) a.u., Ca: 169 ± 17 a.u., Sr: 186 ± 15 a.u., and Ba: 268 ± 22 a.u.

Molecule	R_e (Å)	α_{zz} (a.u.)	α_{100} (a.u.)	(α_A) (a.u.)
MgLi	3.116	482.1	235.4	235.3(7)
CaLi	3.395	599.4	326.0	333 ± 17
SrLi	3.531	640.0	370.4	350 ± 15
BaLi	3.668	660.5	449.2	432 ± 22

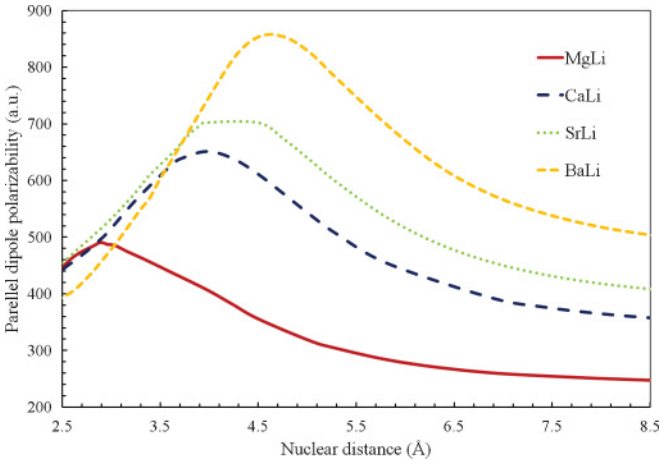

FIG. 3. (Color online) Dipole polarizability of the ground $^2\Sigma$ states for AEM-Li molecules [AEM: Mg (thick red line), Ca (blue long dashed line), Sr (green dotted line), and Ba (orange short dashed line)] (in a.u.) at CCSD(T) levels of correlation.

Using the potential curves in Fig. 1, we solved the vibrational Schrödinger equations and obtained 15, 22, 23, and 26 vibrational states for $^{24}Mg^6Li$, $^{40}Ca^6Li$, $^{88}Sr^6Li$, and $^{138}Ba^6Li$, respectively. Table V shows the energy levels, rotational constants, and PDMs of the lowest vibrational levels ($\nu = 0$–4). We also have tabulated in Table VI the TDMs between the lowest five vibrational states in the electronic ground state. From these data we evaluated the spontaneous emission and black body absorption and emission rates, as shown in Table VII. We took the surrounding environment to be 300 K for the black body radiation calculation. We calculate the lifetimes of the vibrational states by simply taking the inverse of the spontaneous and black body transition rates, which are tabulated in Table VII. To understand the relation between the spontaneous and black body transition rates for low- and high-lying vibrational levels, we tabulated and compared the transition rates for $^{24}Mg^6Li$ from $\nu = 0$ to $\nu = 15$ in Table VIII. It is evident that for the low-lying vibrational levels, spontaneous transition rates are small and hence the lifetimes of these vibrational states are limited by the black body lifetimes. In contrast, for high-lying vibrational levels the spontaneous transition rates becomes larger (corresponding to shorter lifetimes) due to large contributions from overtone ($\Delta\nu = 2$ and $\Delta\nu = 3$) transitions, which in turn is due to anharmonicity of the potential.

Using the total radiative transition rates, we obtained the lifetimes of the vibrational states and plotted that against vibrational quantum number v, as shown in Fig. 4. For all AEM-Li molecules, we find that lower vibrational levels have longer lifetimes than the higher vibrational levels. Also, the lifetimes for lower vibrational levels appear to differ greatly from each other in comparison with higher vibrational levels.

TABLE V. Vibrational energy levels (cm^{-1}), rotational constants (cm^{-1}), and permanent dipole moments (debye) for low-lying vibrational levels.

Molecule	ν	Energy (cm^{-1})	B (cm^{-1})	PDM (debye)
$^{24}Mg^6Li$	0	89.70	0.354	0.860
	1	259.67	0.340	0.785
	2	415.58	0.325	0.710
	3	557.34	0.301	0.642
	4	684.82	0.293	0.577
$^{40}Ca^6Li$	0	98.25	0.276	1.099
	1	297.03	0.272	1.047
	2	489.53	0.265	0.983
	3	666.26	0.255	0.906
	4	830.64	0.250	0.862
$^{88}Sr^6Li$	0	99.98	0.232	0.311
	1	285.76	0.226	0.285
	2	459.62	0.222	0.264
	3	622.76	0.217	0.245
	4	779.83	0.211	0.227
$^{138}Ba^6Li$	0	97.78	0.215	−0.373
	1	289.33	0.212	−0.377
	2	479.47	0.209	−0.380
	3	665.03	0.205	−0.379
	4	843.70	0.201	−0.377

TABLE VI. Transition dipole moments (TDMs) (in debye) between the lowest five vibrational states of each molecule.

	TDM (debye)			
ν–ν'	$^{24}Mg^6Li$	$^{40}Ca^6Li$	$^{88}Sr^6Li$	$^{138}Ba^6Li$
1–0	0.174	0.126	0.037	0.013
2–0	0.052	0.013	0.001	0.006
2–1	0.229	0.197	0.061	0.021
3–0	0.020	0.008	0.001	0.004
3–1	0.089	0.040	0.003	0.009
3–2	0.257	0.241	0.076	0.027
4–0	0.009	0.010	0.002	0.002
4–1	0.041	0.010	0.002	0.007
4–2	0.120	0.076	0.012	0.012
4–3	0.267	0.276	0.085	0.035

TABLE VII. Spontaneous and black body radiation–induced transition rates at $T = 300$ K (in s^{-1}) of the five lowest vibrational excited states of each molecule.

	Spontaneous transition rate (s^{-1})			
ν	$^{24}Mg^6Li$	$^{40}Ca^6Li$	$^{88}Sr^6Li$	$^{138}Ba^6Li$
1	0.046	0.039	0.004	0.001
2	0.090	0.088	0.008	0.003
3	0.134	0.127	0.011	0.008
4	0.176	0.191	0.015	0.014
	Black body transition rate (s^{-1})			
ν	$^{24}Mg^6Li$	$^{40}Ca^6Li$	$^{88}Sr^6Li$	$^{138}Ba^6Li$
0	0.046	0.026	0.003	0.001
1	0.121	0.087	0.009	0.003
2	0.183	0.152	0.015	0.006
3	0.237	0.200	0.021	0.010
4	0.281	0.260	0.026	0.013

TABLE VIII. Spontaneous and black body radiation–induced transition rates at $T = 300$ K (in s^{-1}) of all vibrational states of $^{24}Mg^{6}Li$.

Vibrational number	Spontaneous transition rate	Black body–induced transition rate
0	–	0.046
1	0.046	0.121
2	0.090	0.183
3	0.134	0.237
4	0.176	0.281
5	0.219	0.303
6	0.261	0.292
7	0.303	0.251
8	0.346	0.201
9	0.387	0.156
10	0.421	0.126
11	0.450	0.108
12	0.462	0.095
13	0.448	0.082
14	0.404	0.067
15	0.307	0.047

As discussed earlier, we see an inverse relationship between the PDM values and the lifetimes of vibrational states. The PDMs are smaller and the lifetimes longer for SrLi and BaLi compared to those for MgLi and CaLi. Lifetimes of the lowest vibrational state ($\nu = 0$ and $J = 0$) were found to be 22, 39, 380, and 988 s for $^{24}Mg^{6}Li$, $^{40}Ca^{6}Li$, $^{88}Sr^{6}Li$, and $^{138}Ba^{6}Li$, respectively. To quantify the uncertainty in the lifetime of lowest vibrational states, we need to know the accuracy of our PDM values. However, there is no experimental value for the AEM-Li systems. Hence we calculated the PDM of the LiF molecule with the present method [CCSD(T)–ANO-RCC]. Comparison with available experimental PDM (6.284 D [46]) at the equilibrium distance and our CCSD(T) estimate (6.08 D), the uncertainty in PDM is found to be less than 3%. If we assume the uncertainty in AEM-Li systems to be of similar order to LiF, the lifetime uncertainties are estimated to be less than 10%. We also assume the energy uncertainty is similar to R_e uncertainty (∼1%) in the above estimate. Lifetimes of higher vibrational states may not be accurate as TDMs and energies depend greatly on fitting parameters. Lifetimes of the lowest excited rotational level ($\nu = 0$, $J = 1$) were found to be longer than the vibrational lifetimes by several orders of magnitude, mainly due to the small energy difference between the $J = 0$ and $J = 1$ level. We found the rotational lifetimes to be 1.2×10^7 s, 1.5×10^7 s, 32.4×10^7 s, and 27.5×10^7 s for $^{24}Mg^{6}Li$, $^{40}Ca^{6}Li$, $^{88}Sr^{6}Li$, and $^{138}Ba^{6}Li$, respectively. Although our estimated vibrational lifetimes are shorter than the rotational lifetimes, they are sufficient for ultracold experiments, such as long-range dipole-dipole interactions and precise measurements for testing time variance of the proton-to-electron mass ratio [44].

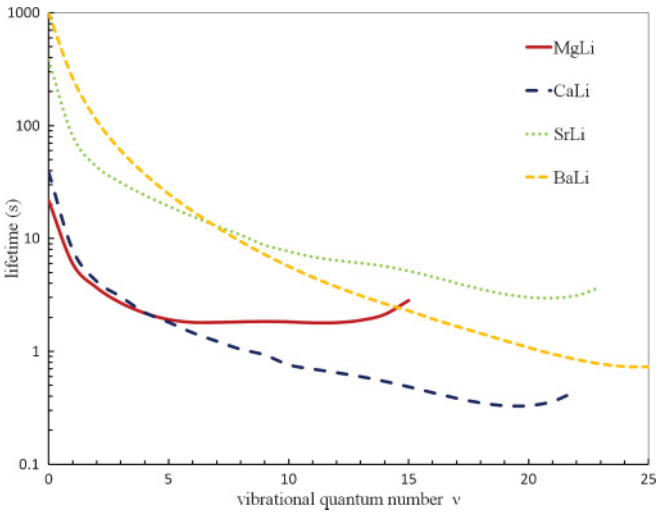

FIG. 4. (Color online) Lifetimes of $J = 0$ vibrational states taking both spontaneous and black body–induced transition at $T = 300$ K for AEM-^{6}Li molecules [AEM: Mg (thick red line), Ca (blue long dashed line), Sr (green dotted line), and Ba (orange short dashed line)] at CCSD(T) levels of correlation.

IV. CONCLUSIONS

In this paper we have presented the *ab initio* calculations of the electronic ground state ($^2\Sigma$) of AEM-Li (AE: Mg, Ca, Sr, and Ba) systems. These systems are good candidates for the study of anisotropic long-range dipole-dipole interactions in ultracold experiments. First, we investigated the potential energy curves and spectroscopic constants of the electronic ground state at the CCSD(T) level. We used the third-order Douglas-Kroll spin-free Hamiltonian and ANO-RCC basis sets. The calculated spectroscopic constants were in good agreement with previous theoretical and experimental results (∼1%).

Second, we obtained the electronic ground-state PDM functions at the CCSD(T) level using the FFPT method to evaluate the strength of the dipolar interactions. The obtained PDM values at the equilibrium internuclear distance were reasonably large, especially for MgLi (0.90 D) and CaLi (1.15 D). Hence, these molecules might be better candidates for the study of long-range dipole-dipole interactions. We checked the reliability of the PDM curve by performing a 100.0 a.u. calculation and finding the PDM to be zero, as expected at atomic limits. In addition, a recent paper [47] on potential energy curves and PDMs of alkaline-earth-metal–Li systems shows a similar trend (except for the differences in the PDMs at small distances), adding to the reliability of the results. We also investigated the ground-state electric dipole polarizability over the internuclear distance. We compared the calculated dipole polarizability, obtained at 100.0 a.u., to the sum of atomic polarizabilities. We found very close agreement (less than 1%) between our supermolecular polarizabilities and atomic polarizabilities for all the molecules.

Finally, we obtained the vibrational wave functions from the potential energy curves and computed transition dipole moments at the vibrational level. From the vibrational energies and transition dipole moments we evaluated the black body ($T = 300$ K) and spontaneous transition rates of the five lowest vibrational states. The obtained radiative lifetimes for the

$\nu = 0$ vibrational state were at least 20 s, sufficiently large for ultracold experiments. Within a fair approximation, the uncertainty of the lifetimes of low-lying vibrational states is estimated to be less than 10%.

ACKNOWLEDGMENTS

G.G. and M.H. thank the Center for Research in Emerging Science and Technology (CREST). One of the authors, M.A., thanks the Japan Society for the Promotion of Science.

[1] M. H. Anderson, J. R. Ensher, M. R. Matthews, C. E. Wieman, and E. A. Cornell, Science **269**, 198 (1995).
[2] C. S. Adams, M. Sigel, and J. Mlynek, Phys. Rep. **240**, 143 (1994).
[3] C. Menotti, M. Lewenstein, T. Lahaye, and T. Pfau, AIP Conf. Proc. **970**, 332 (2008).
[4] L. Santos, G. V. Shlyapnikov, P. Zoller, and M. Lewenstein, Phys. Rev. Lett. **85**, 1791 (2000).
[5] E. R. Meyer, J. L. Bohn, and M. P. Deskevich, Phys. Rev. A **73**, 062108 (2006).
[6] T. Zelevinsky, S. Kotochigova, and J. Ye, Phys. Rev. Lett. **100**, 043201 (2008).
[7] M. Kajita, New J. Phys. **11**, 055010 (2009).
[8] S. Kotochigova, P. S. Julienne, and E. Tiesinga, Phys. Rev. A **68**, 022501 (2003).
[9] K. K. Ni, S. Ospelkaus, M. H. G. de Miranda, A. Peter, B. Neyenhuis, J. J. Zirbel, S. Kotochigova, P. S. Julienne, D. S. Jin, and J. Ye, Science **322**, 231 (2008).
[10] N. Mabrouk and H. Berriche, J. Phys. B **41**, 155101 (2008).
[11] C. Haimberger, J. Kleinert, O. Dulieu, and N. P. Bigelow, J. Phys. B **39**, S957 (2006).
[12] G. Gel-Mann, U. Wedig, P. Fuentealba, and H. Stoll, J. Chem. Phys. **84**, 5007 (1986).
[13] S. Kotochigova and E. Tiesinga, J. Chem. Phys. **123**, 174304 (2005).
[14] J. M. Sage, S. Sainis, T. Bergeman, and D. DeMille, Phys. Rev. Lett. **94**, 203001 (2005).
[15] L. K. Sorensen, T. Fleig, and J. Olsen, J. Phys. B **42**, 165102 (2009).
[16] J. Deiglmayr, A. Grochola, M. Repp, K. Mortlbauer, C. Gluck, J. Lange, O. Dulieu, R. Wester, and M. Weidemuller, Phys. Rev. Lett. **101**, 133004 (2008).
[17] W. Stwalley and H. Wang, J. Mol. Spectrosc. **195**, 194 (1999); K. M. Jones, E. Tiesinga, P. D. Lett, and P. S. Julienne, Rev. Mod. Phys. **78**, 483 (2006).
[18] P. Courteille, R. S. Freeland, D. J. Heinzen, F. A. van Abeelen, and B. J. Verhaar, Phys. Rev. Lett. **81**, 69 (1998); S. Inouye, K. B. Davis, M. R. Andrews, J. Stenger, H. J. Miesner, D. M. Stamper-Kurn, and W. Ketterle, Nature (London) **392**, 151 (1998); T. Khler, K. Gral, and P. S. Julienne, Rev. Mod. Phys. **78**, 1311 (2006).
[19] N. Nemitz, F. Baumer, F. Munchow, S. Tassy, and A. Gorlitz, Phys. Rev. A **79**, 061403(R) (2009).
[20] G. Gopakumar, M. Abe, B. P. Das, M. Hada, and K. Hirao, J. Chem. Phys. **133**, 124317 (2010).
[21] P. Zhang, H. R. Sadeghpour, and A. Dalgarno, J. Chem. Phys. **133**, 044306 (2010).
[22] M. Okano, H. Hara, M. Muramatsu, K. Doi, S. Uetake, Y. Takasu, and Y. Takahashi, Appl. Phys. B: Lasers Opt. **98**, 691 (2010).
[23] M. Tomsa, F. Pawlowski, M. Jeziorska, C. P. Koch, and R. Moszynski, Phys. Chem. Chem. Phys. **13**, 18893 (2011).
[24] E. Czuchaj, M. Krosnicki, and H. Stoll, Chem. Phys. Lett. **371**, 401 (2003).
[25] M. Kitagawa, K. Enomoto, K. Kasa, Y. Takahashi, R. Ciurylo, P. Naidon, and P. S. Julienne, Phys. Rev. A **77**, 012719 (2008).
[26] M. Kajita, M. Abe, M. Hada, and Y. Moriwaki, J. Phys. B **44**, 025402 (2011).
[27] M. Abe, M. Kajita, M. Hada, and Y. Moriwaki, J. Phys. B **43**, 245102 (2010).
[28] R. Guerout, M. Aymar, and O. Dulieu, Phys. Rev. A **82**, 042508 (2010).
[29] B. O. Roos, R. Lindh, P. A. Malmqvist, V. Veryazov, and P. O. Widmark, J. Phys. Chem. A **112**, 11431 (2008).
[30] G. Karlstrom *et al.*, Comput. Mater. Sci. **28**, 222 (2003).
[31] N. Douglas and N. M. Kroll, Ann. Phys. **82**, 89 (1974).
[32] B. A. Hess, Phys. Rev. A **33**, 3742 (1986).
[33] C. W. Bauschlicher, S. R. Langhoff, and H. Patridge, J. Chem. Phys. **96**, 1240 (1992).
[34] L. M. Russon, G. K. Rothschopf, M. D. Morse, A. I. Boldyrev, and J. Simons, J. Chem. Phys. **109**, 6655 (1998).
[35] A. R. Allouche and M. Aubert-Frècon, Chem. Phys. Lett. **222**, 524 (1994).
[36] R. Guerout, M. Aymar, and O. Dulieu, Phys. Rev. A **82**, 042508 (2010).
[37] A. R. Allouche and M. Aubert-Frecon, J. Chem. Phys. **100**, 938 (1994).
[38] M. Kajita, G. Gopakumar, M. Abe, and M. Hada, Phys. Rev. A **84**, 022507 (2011).
[39] G. Gopakumar, M. Abe, M. Hada, and M. Kajita, Phys. Rev. A **84**, 045401 (2011).
[40] A. R. Allouche, M. Aubert-Frecon, G. Nicolas, and F. Spiegelmann, J. Chem. Phys. **200**, 63 (1995).
[41] A. Stein, H. Knockel, and E. Tiemann, Eur. Phys. J. D **57**, 171 (2010).
[42] C. R. Vidal, J. Chem. Phys. **72**, 1864 (1980).
[43] C. Linton, F. Martin, I. Russier, A. J. Ross, P. Crozet, S. Churassy, and R. Bacis, J. Mol. Spectrosc. **175**, 340 (1996).
[44] S. Ospelkaus, K. K. Ni, D. Wang, M. H. G. de Miranda, B. Neyenhuis, G. Quemener, P. S. Julienne, J. L. Bohn, D. S. Jin, and J. Ye, Science **327**, 853 (2010).
[45] P. Schwerdtfeger, *Atoms, Molecules and Clusters in Electric Fields - Theoretical Approaches to the Calculation of Electric Polarizability*, edited by G. Maroulis (World Scientific, Imperial College Press, 2009).
[46] L. Wharton, W. Klemperer, L. P. Gold, R. Strauch, J. J. Gallagher, and V. E. Derr, J. Chem. Phys. **38**, 1203 (1963); A. J. Herbert, F. J. Lovas, C. A. Melendres, C. D. Hollowell, T. L. Story Jr., and K. Street Jr., *ibid.* **48**, 2824 (1968).
[47] S. Kotochigova, A. Petrov, M. Linnik, J. Klos, and P. S. Julienne, J. Chem. Phys. **135**, 164108 (2011).